Separation of Fundamental Wave and Transient Components of the Current Signal for Machine Insulation State Monitoring

C. Zoeller, Th. Winter and Th.M. Wolbank
Institute of Energy Systems and Electrical Drives,
Vienna University of Technology
Vienna, Austria

M.A. Vogelsberger and M. Bazant*
GSC/PPC-Drives VI
Bombardier Transportation Austria GmbH
Vienna, Austria
*Bombardier Transportation (Switzerland) Ltd.

***Abstract*—In this work a method to detect insulation degradation of an adjustable speed drive (ASD) based on analyses of the transient current reaction caused by inverter switching is proposed. The drive system consists of an inverter fed three phase induction machine with 1.4MW. The standard current sensors are used to analyze the transient signal ringing to extract an insulation state indicator of the winding system and for the control of the machine as well. Using the inverter as a source of excitation, it is possible to perform an insulation test by evaluation of the resulting transient current sensor signals. The influences of the fundamental wave portion and transient component of the current signal on the insulation state indicator are analyzed. An effective separation of these components is investigated with an algorithm applicable for real time evaluation of the insulation state.**

Keywords—AC machines; fault diagnosis; insulation; electric breakdown, current sensors

I. INTRODUCTION

The demand of monitoring systems to prevent breakdowns of modern drive systems is continuously increasing. Due to speed variability, dynamics and robustness, adjustable speed drives (ASD) are the first choice for many applications, for example in safety-critical applications as well as in public and cargo transportation systems. In both fields the breakdown of a drive is linked with high economic costs and significant loss of image. Stator related faults are with a probability of 35%, the second most common faults, causing a machine outage [1]-[2]. About 70% of these outages are caused by faulty the stator insulation system.

An overview of the technical details and structure of stator insulations is described in [3]. Regarding larger machines with nominal power of few MW, the stator insulation system mainly consists of the components strand, turn and groundwall insulation. At random-wound machines, the strand insulation can function as the turn insulation and only in key areas additional insulation exists. Determining the winding condition and expectation of the remaining life is a common reason for testing the drive system. In addition with a high number of drive systems in operation, the expenditure of time and resources have to be carefully considered and prioritized maintenance will be necessary. Most industrially applied monitoring techniques can only be applied offline. Offline insulation monitoring methods which are often described in the context of insulation degradation are e.g. polarization index PI [4], dissipation factor tan δ [5], partial discharge (PD) [3], DC/AC HiPot [3] or capacitance tests using a capacitance bridge or a vector network analyzer. All these tests have in common that special equipment and knowledge is needed.

In literature different stresses like electrical, thermal, thermo-mechanical and mechanical are considered responsible for a reduced insulation lifetime [3]. One of the most important degradation mechanisms is thermo-mechanical stress due to load changes or on-off operation. The insulation system is aged due to different thermal expansion coefficients of the materials and temperature gradients inside the machine. Usually the process of insulation degradation is proceeding very slowly, sometimes even over decades. This offers the possibility to monitor the insulation state over years analyzing the trend of degradation. Investigations on coil specimen, representing stator segments, show that thermal-electrical aging realized through a high number of operating hours with temperatures above the upper-limiting temperature (specified for the insulation class) and vibration exposure causes a change in the capacitance value of the specimen [6]-[7]. According to [8] a change in the turn-turn capacitance of a form wound coil resulting from stress through thermal cycling is detectable. The capacitance is in all cases usually considered as the dominant parameter for insulation health state evaluation. Usually a heavily degraded insulation at first leads to a turn to turn fault and finally to severe ground fault as described in [9]. With inverter-fed machines the insulation is strained by the high voltage change rates and occurring overvoltage through cable impedance mismatch, which can reach 2-4 times the DC-link voltage [10]. This can further accelerate the insulation degradation process.

Many approaches aims to detect a fault, which is already present. With frequency domain techniques, especially ones based on fast Fourier transforms (FFT) fault diagnoses of electric machines are possible, as described in [11]. For instance, motor current signature analysis (MCSA), is applied to detect possible stator inter-turn faults. This method analyses the line current harmonics of the measured current signals. Another approach that analyses the terminal voltage harmonics

The work to this investigation was supported by the Austrian Research Promotion Agency (FFG) under project number 83 84 78.

requires additional voltage sensors, often not available in modern drives.

In [12] stator insulation condition monitoring for failure-prone inverter-fed machines, whenever the motor is under operation, is given. The main concept of the proposed technique is to apply a DC and/or variable frequency AC test voltage to the stator insulation using the inverter, to perform standard off-line insulation tests. Through detecting changes in the leakage current of the system the groundwall insulation state is analyzed.

In [13] insulation condition monitoring only based on the current sensors signals for a 5.5kW induction machine is shown. The technique is based on analysis of the transient part of the current sensor signals after voltage step excitation through a switching transition of the inverter e.g. from lower short-circuit to active switching state. The same sensors are also used for the control of the machine. Resulting to this excitation of the single phases, changes in the transient signal shape of the current sensors are detectable, depending on the actual insulation health state. In this paper the proposed method is tested for a 1.4MW induction machine and the possible interaction with the fundamental wave behavior is investigated. Additionally, the implementation of necessary signal preprocessing steps is analyzed regarding the computational burden and real time applicability to effectively separate the transient components that are exploited for the insulation health state monitoring from disturbing influences through the machines fundamental wave behavior.

II. Essentials of the Proposed Monitoring Method

The insulation health state monitoring method is based on analysis of the transient current reaction to a step voltage excitation of the machine winding. With the inverter, every phase can be excited separately. The fast rising voltage steps in combination with the improper terminated supply cables from the inverter to the machine cause transient overvoltage on the end of the line. This ringing with exponential decaying behavior is also observable in the current sensors response to the step excitation. In Fig. 1 the first 50μs of the current reaction (solid blue) to a step excitation is shown.

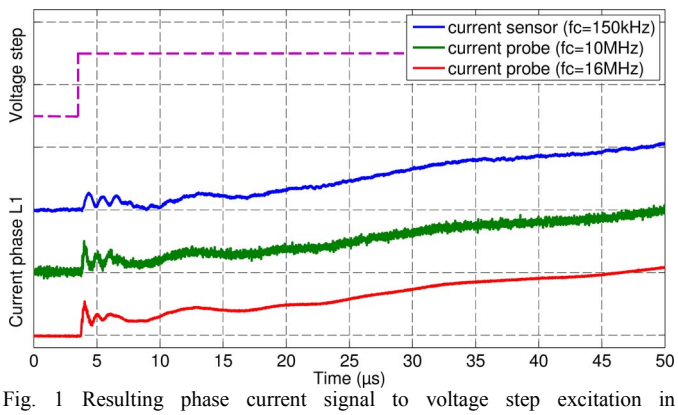

Fig. 1 Resulting phase current signal to voltage step excitation in corresponding phase.

The current trace is recorded with a standard industrial current sensor with a specified bandwidth of DC-150 kHz and a maximum di/dt of 50A/µs. Though the frequencies appearing in the transient current response are partly outside the specified frequency range, the signal still contains useful information on changes in the insulation system. Additionally, two different current probes with a cutoff frequency specification of 10MHz (green trace) and 16MHz (red trace) are recorded. The transient part of the current reaction is clearly visible within the first 20µs of all three sensor systems applied. A sampling rate of 120 MS/s is used for the measurements analyzed in this paper. The duration of the transient ringing depends on different factors, e.g. the inverter switching time, supply voltage level, cabling between inverter and machine and the machine itself. The drive system consists of three main components, the inverter, cabling and the machine as depicted in Fig. 2, illustrating a switching transition in phase L1 from lower short circuit to an active state. These three main components form a complex system. The characteristic of the fast voltage step depends on the inverter technology used.

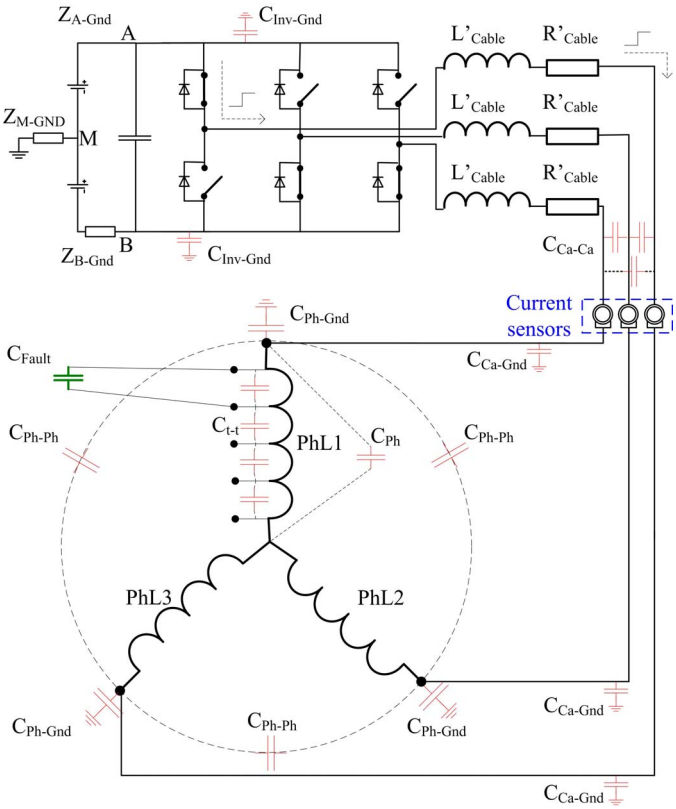

Fig. 2 Schematic view of the complex system inverter, cabling and machine with parasitic capacitances and fault component.

A capacitive coupling of inverter to ground exists, denoted with $C_{Inv\text{-}Gnd}$ influencing the whole system behavior. The cabling can be represented with the characteristic impedance, the resistances R_{cable}' and inductances L_{cable}' per unit length, and the capacitances cable to ground $C_{Ca\text{-}Gnd}$ and cable to cable $C_{Ca\text{-}Ca}$, as indicated. And finally the machine, with the parasitic elements phase to phase $C_{Ph\text{-}Ph}$, phase to ground $C_{Ph\text{-}Gnd}$, turn to turn $C_{t\text{-}t}$ and the total phase capacitance C_{Ph}. All these elements influence the electrical high frequency behavior of the machine at voltage step excitation and thus the transient current reaction. Because the insulation degradation is always linked with a capacitive change, the externally placed fault

capacitor C_{Fault} is also depicted in the figure. This emulates a change in the capacitive characteristic of the machine, and hence a deviation to the healthy machine is observable in the transient part of the current sensor reaction.

A. Measurements and fundamentals of the method

The measurements are conducted on a test stand with a special type 1.4 MW induction machine with tappings. With this setup, insulation degradation is emulated with capacitances placed parallel to the winding or coils, forcing a change of the impedance characteristic of the machine. To get a rough knowledge of the values of the involved parasitic capacitances the machine's phase-to-ground capacitance $C_{ph\text{-}gnd}$ is determined to 63nF. A high number of tappings in phase L1 and L2 exist to facilitate the investigations of different insulation degradation scenarios. The change in the impedance characteristic affects the current reaction after a step excitation is applied. This deviation is compared with a reference measurement of the same machine in a healthy machine state (without additional capacitance). In Fig. 3, a comparison of the current response in case of the healthy machine (blue) and with emulated insulation degradation with a capacitor of 7.5nF parallel to the whole phase L1 is shown using industrial current sensors with bandwidth of 150kHz. The deviation between both traces is clearly observable. The measured current responses of a phase after step excitation with different machine conditions, regarding the insulation state, show characteristic deviations suitable for an insulation state evaluation.

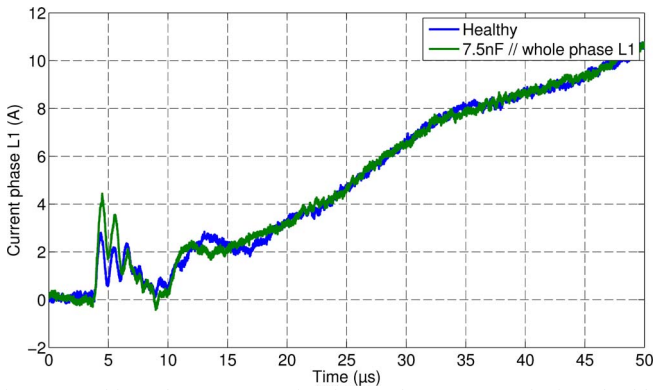

Fig. 3 Resulting phase current signal to voltage step excitation; healthy machine (blue); emulated insulation degradation (green); sensor bandwidth 150kHz.

Before the measured current signals are subsequently analyzed, further signal preprocessing steps are necessary. A trigger detection algorithm is used to determine the accurate instant of the rising edge of the current. Thus, influences through possible jitter in the inverter output waveform are avoided. Furthermore, the mean signal slope is calculated and is subtracted. The mean current slope is determined by the machines transient leakage inductance that in turn is influenced by inherent machine asymmetries like slotting. An example of the described signal processing (upper figure – measured current reaction) and the result of the time signal after preprocessing (lower figure) is depicted in Fig. 4.

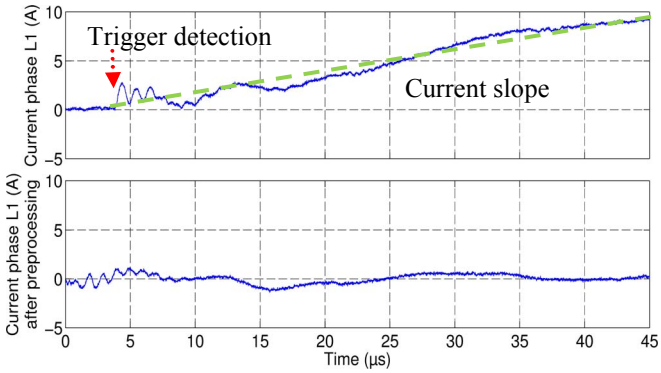

Fig. 4 Procedure of the signal preprocessing (upper figure – original signal) and resulting signal (lower figure).

After preprocessing, the signal is analyzed in the frequency domain by applying the fast Fourier transformation. To enable statistical analyses a higher number of consecutive single measurements is carried out to represent one machine state (about 33). The mean of the resulting spectra for the healthy machine condition (blue trace), the emulated insulation degradation with 7.5nF placed parallel to the 1st coil of phase L1 (green trace) and the square deviation of both traces (dashed red) are shown in Fig. 5 a).

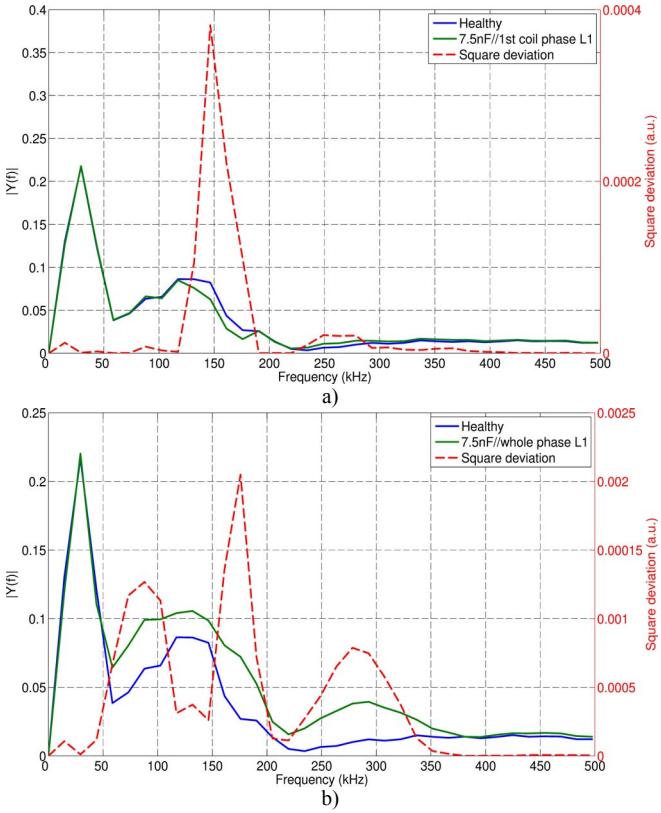

Fig. 5 Spectra of current signal a) healthy (solid blue) and fault scenario 7.5nF//1st coil phase L1 (solid green) and b) healthy (solid blue) and 7.5nF//whole phase L1(solid green); square deviation (dashed red)

Subfigure b) depicts the comparison between the healthy machine and the fault scenario 7.5nF parallel to the whole phase L1, thus representing a degradation with higher severity. The blue trace serves as a reference and represents the first

measurement of the new machine after initial operation of the drive system. A change of the green trace (representing measurements e.g. taken after several operation hours) with respect to the reference can then be interpreted as insulation degradation. The frequency range significant for insulation degradation is selected from 50 kHz to 500 kHz. Below 50 kHz the magnitude values of the analyzed spectra are occasionally subjected to higher fluctuations and inaccurateness in the current slope estimation that affect this low frequency range. As part of the frequency range of interest is outside the specification of the current sensors, their signal accuracy is clearly reduced. However their transfer functions are still reproducible. Similar signal deviations are approved with the additional current probes having higher cutoff frequencies. The most noticeable change of the frequency spectrum depends on the severity and location of the degradation. If the degradation affects the whole phase, the degradation is observable over a wide range from 50kHz to 350kHz. In case of a single coil degradation the range can be quantified from 100kHz to 200kHz. Therefore the whole frequency range mentioned before is analyzed. The Root Mean Square Deviation (RMSD) calculated from the difference of the reference spectrum and spectra of further measurements has been found a good indicator to express the severity of the insulation change and the insulation state is expressed with this indicator, denoted ISI in the following. With equation (1) the RMSD between two traces is calculated.

$$ISI_p = RMSD_p(x_1, x_2) = \sqrt{\frac{\sum_{i=1}^{n}\left(Y_{ref,p}(f_i) - Y_{con,p,k}(f_i)\right)^2}{n}} \quad (1)$$

$$x_1 = Y_{ref,p} = \frac{\sum_{k=1}^{m} Y_{ref,p,k}}{m};\ x_2 = Y_{con,p,k} \quad (2)$$

The index p identifies the investigated phase. The variable $Y_{ref,p}$ represents the mean of a set of amplitude spectra calculated out of a set of reference measurements. The variable $Y_{con,p,k}$ is the amplitude spectrum of later measurement. The index k represents the consecutive number of repeated measurements. The variable n depends on the time window length. To enable statistical analyses and to increase the accuracy, the quantity of spectra for the mean is set to a higher number (Index m), see equation (2). The consecutive measurements are done with a real-time system and two FPGA modules (inverter control and measurement unit). The minimum system requirements and investigations on additional disturbing influences (e.g. cabling length, temperature and moisture) are described in [14]-[15].

III. Testing the Insulation Health State

Different scenarios are tested to verify the sensors performance and the proposed signal processing. A small impedance change is stimulated by a capacitance, placed parallel to the first single coil of totally twelve in one phase. A high change is provoked with a capacitance parallel to the whole phase. Different capacitances with 3nF, 7.5nF and 15nF were tested. In Fig. 6 the calculated ISI values (for phase L1) for different fault scenarios in the corresponding phase for all three used sensor types are depicted. It is visible that the indicators determined with the three sensors separately, show a monotonic increasing tendency for higher severity. All tested scenarios deliver higher indicator values compared to the reference (healthy) case and are thus indicating insulation degradation.

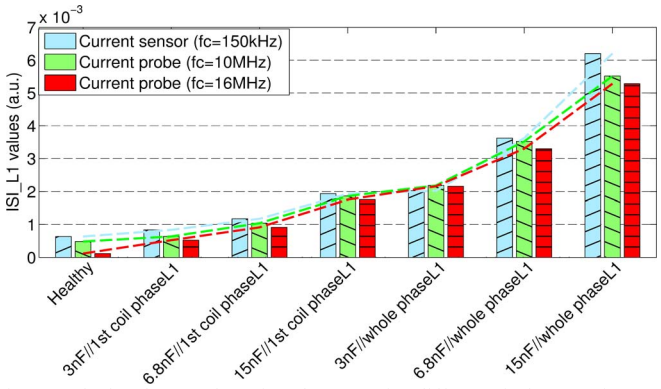

Fig. 6 Calculated ISI values for phase L1 for different fault scenarios and sensors.

If a change in the high-frequency behavior is affecting only one phase, the indicator will increase only for this specific phase. With a linear combination of the three phase indicators, each representing the state for the corresponding phase, it is possible to identify the location of this asymmetry. Furthermore the effect of possibly disturbing influences like temperature and humidity occurring symmetrically in all three phases can thus be reduced. With equation (3) the spatial indicator SISI is given.

$$SISI = ISI_{L1} + ISI_{L2} * e^{\frac{j2\pi}{3}} + ISI_{L3} * e^{\frac{j4\pi}{3}} \quad (3)$$

In Fig. 7 the spatial location of the detected insulation degradation for different scenarios are shown.

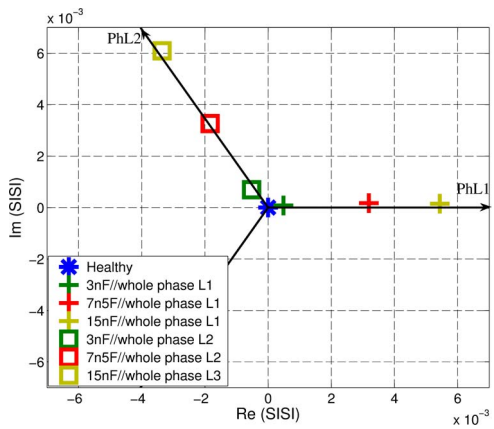

Fig. 7 Spatial representation of analyzed fault scenarios.

IV. Analysis of Signal Preprocessing

A. Influence of fundamental wave signal components

This section examines how the slope of the time signals affects the components of the amplitude spectrum and as a result the insulation health state indicator. The slope is determined by the transient leakage inductance of the machine

as can be seen in the voltage stator equation in space phasor representation, with the stator resistance r_S, the leakage induction l_l times the current time derivative and time derivative of rotor flux $\underline{\lambda}_R$ (back electromotive force).

$$\underline{v}_s = r_s \underline{i}_s + l_l \frac{d\underline{i}_s}{d\tau} + \frac{d\underline{\lambda}_R}{d\tau} \quad (4)$$

Due to inherent asymmetries of the machine (e.g. slotting, saturation effects) this reactance is not constant, leading to a rotor position depending modulation. These fundamental wave signal components do not contain information for the insulation state estimation. To illustrate the influence of the current slope Fig. 8 a) depicts the spectrum of the current response, after all signal preprocessing steps are done, in comparison to the spectrum only of the current slope depicted in subfigure b).

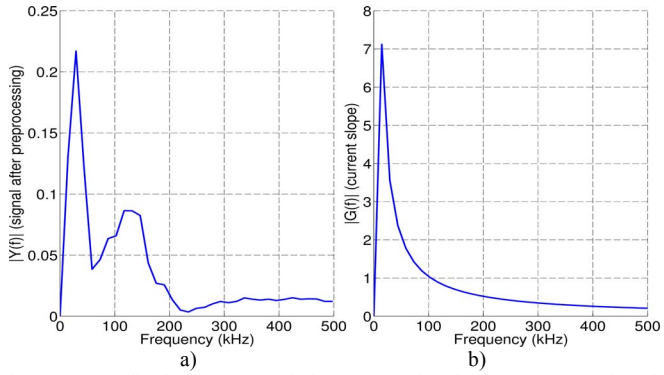

Fig. 8 a) Amplitude spectrum of the current signal after preprocessing, b) spectrum of the current slope.

As can be seen, the spectrum of the current slope (right subfigure) shows components over the whole frequency range with magnitudes several higher than of the preprocessed signal (left subfigure). Thus, the frequency components of the slope are eliminated by subtraction of the mean current slope, as described in Fig. 4. Furthermore, the correct estimation of the current slope is essential to ensure the accuracy of the insulation monitoring method. In Fig. 9 a single current reaction in case of emulated insulation degradation with 7.5nF in parallel to the first coil (blue trace) with the estimated mean current slope (solid green trace) is shown. The red trace represents the current reaction after subtraction of the mean current slope. With an assumption of a wrong estimated slope (calculation error +10%, dashed green trace), again the difference is calculated (amber trace). The spectra of the two preprocessed current reactions (red and amber trace) are calculated and the RMSD to the reference data shows the deviation to the healthy machine state. This procedure is repeated for an assumed slope error of +20% and +30% and in case of the emulated insulation degradation with 7.5nF parallel to the whole phase L1, with the results of the RMSD depicted in Fig. 10. As can be seen, the influence is not negligible and the accuracy of the slope calculation influences the sensitivity of the health state indicator.

To analyze the statistical behavior, the influence of the error is simulated with a random function and the slope factor is modified up to +10% and +20% separately for 33 measurements.

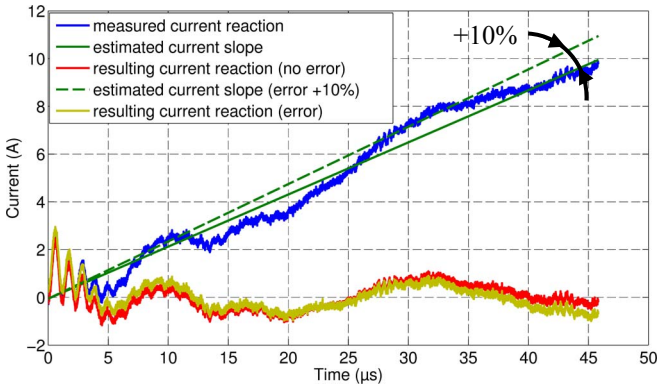

Fig. 9 Current reaction induced by step excitation (blue) with estimated slope (green) and resulting signal after subtraction (red) compared to the same data with a slope error of +10% (dashed green and amber).

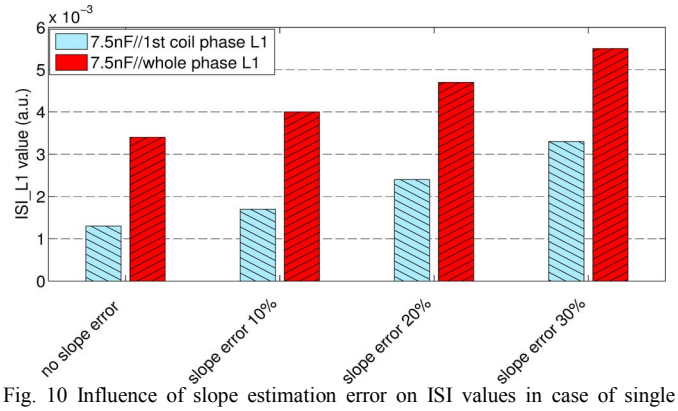

Fig. 10 Influence of slope estimation error on ISI values in case of single measurements with different emulated insulation degradation.

The measurements of phase L1 if a voltage step excitation is applied to the same phase have been carried out at standstill. As the rotor has not be turned and attached load is not an issue during the measurement the steady state value of the current time derivative is the same in all 33 measurements. Fig. 11 a-c) depict the results for different emulated insulation degradation scenarios and possible slope errors in the so-called box plot. Different capacitances (3nF, 7.5nF and 15nF) were separately placed parallel to the first coil of phase L1 or whole the phase L1. For every machine condition 33 single measurements are recorded and with the spectra, the ISI values are calculated. The box plot representation gives a statistical statement about the distribution of the indicators. Within the blue box 50% of the values are located and the red line represents the median of the data set. Increasing values for increasing insulation degradation implicates that all tested scenarios are distinguishable from the first box plot representing the healthy machine state (no overlap exists). In subfigure a) the fault scenarios are analyzed with no artificial slope error. The boxes are concentrated around their median values and all faulty machine conditions are separable from the healthy machine state. In subfigure b) and c) the same measurements are analyzed with a possible slope error of 10% respectively 20%.

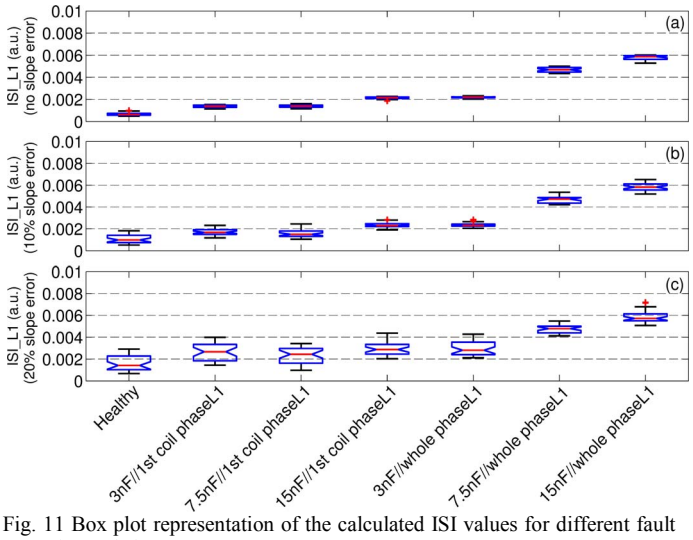

Fig. 11 Box plot representation of the calculated ISI values for different fault scenarios and slope errors.

As can be seen in the figure, all boxes are enlarged in subfigure b) and c). The error in the estimated slope thus influences the accuracy of the proposed insulation monitoring method. With an accurate signal slope calculation and a high number of measurements no loss of sensitivity exists.

In the following section a recursive approach based on the least square method for the current slope estimation is investigated. This algorithm is tested for the real-time estimation of the current slope and investigated regarding the computational burden.

B. *Current slope estimation with least square method*

The least squares method is based on an over determined system of linear equations of the form

$$y = Sp \tag{5}$$

with the *(m x n)*- matrix *S* (data matrix), the *m* dimensional vector *y* (output sequence) and the unknown *n* dimensional vector *p* (parameter vector). There is no solution for *p* in equation (5) if *m>n* and *rank(S)=n≠rank([S,y])*. The solution p_0 which minimizes the square deviation $\min_p \|\boldsymbol{e}\|_2^2$ with *e=y-Sp* is the optimal solution, given with equation (6).

$$p_0 = (S^T S)^{-1} S^T y \tag{6}$$

For the calculation of the parameter vector p_0 the entire vector *y* and the pseudo inverse $(S^T S)^{-1} S^T$ is needed. With *N*+1 measurements the equation *e=y-Sp* can be enhanced to equation (7) with the estimation of parameter vector $\hat{p}$.

$$\begin{bmatrix} e_0 \\ \vdots \\ e_{N+1} \end{bmatrix} = \begin{bmatrix} y_0 \\ \vdots \\ y_{N+1} \end{bmatrix} - \begin{bmatrix} s_0^T \\ \vdots \\ s_{N+1}^T \end{bmatrix} \hat{p}_{N+1} \tag{7}$$

Because of the increasing size of *y* and *S*, this method is not suitable for real-time applications.

For real-time estimation of the slope, a recursive algorithm is thus desirable. Such an algorithm process only one data value per iteration and calculates an estimation of the slope and offset. With each measured value, the calculated slope and the offset are updated. This approach saves the amount of memory needed and reduces calculation time. For *j*=0,..,*N*+1 measurements and equation (6) the optimal solution is stated with equation (8)

$$\hat{p}_{N+1} = (S_{N+1}^T S_{N+1})^{-1} S_{N+1}^T y_{N+1} \tag{8}$$

Inserting and splitting of the data matrix $S_{N+1} = (S_N, s_{N+1}^T)^T$ and $y_{N+1} = (y_N, y_{N+1})^T$ in equation (8) and resolving the matrix inversion, the following equations (9),(10) and (11) with the substitution of $P_N = (S_N^T S_N)^{-1}$ for the estimation problem are obtained.

$$h_{N+1} = \frac{P_N s_{N+1}}{(1 + s_{N+1}^T P_N s_{N+1})} \tag{9}$$

$$P_{N+1} = P_N - h_{N+1} s_{N+1}^T P_N \tag{10}$$

$$\hat{p}_{N+1} = \hat{p}_N + h_{N+1}(y_{N+1} - s_{N+1}^T \hat{p}_N) \tag{11}$$

There still remains the question of suitable starting values for P_N and $\hat{p}_N$. With the selection of $P_N = \alpha E$ (with α=10000 and *E* as the unit matrix) the estimation values show accurate results. The starting value for $\hat{p}_N$ is usually set to zero or to the nominal value of the parameter to be estimated, if known. To calculate the slope *k* and the offset *d* of an equation of a straight line $g = kx + d$, in which more than two points are given, the least squares method can be applied with $s^T = (x, 1)^T$ with the known sampled values *x* and $p = (k, d)^T$. A further simplification step is to calculate the current slope after the first 20μs if the transient part of the signal decayed. This approach reduces the computational burden and also delivers accurate values.

In Fig. 12 the mean of the current reaction for a step excitation in phase L1, the mean of the calculated current slope of the recursive least square algorithm and the mean of the calculated current slope with a non recursive robust regression is depicted.

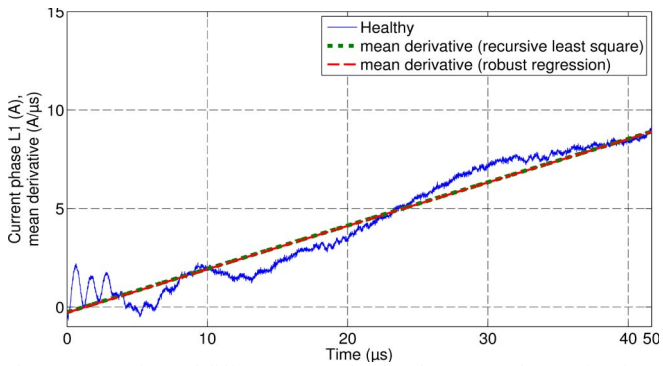

Fig. 12 Comparison of different approaches for the current slope estimation.

In Table 1 the mean slope factor value of 33 measurements for both used regression methods are shown.

TABLE 1 RESULTS OF THE PARAMETER FOR DIFFERENT IMPLEMENTATIONS

	Recursive Least Square Regression	***Robust Regression***
Slope factor *k*	$1.8317*10^{-3}$	$1.8361*10^{-3}$
Variance	$1.0020*10^{-12}$	$8.6500*10^{-13}$

The deviation is negligible and the variance is very low for both functions. The recursive least square approach delivers

results with accuracy high enough to separate the fundamental wave signal components and the interesting transient ringing used for the insulation monitoring method.

V. CONCLUSION

A method to detect insulation degradation of three phase ac machines based on the information of the current sensors has been presented. The proposed technique is based on evaluating the current transients resulting from step voltage excitation. These transients are mainly influenced by the drive's parasitic capacitive components and insulation degradation is always linked with a change of this capacitance that is considered the dominant parameter for insulation health state evaluation. The time signals of the current reactions are transferred into frequency domain by applying the fast Fourier transformation and based on the deviation between reference measurement at initial operation of the drive and later in-service measurements, information about the insulation condition is obtained. Measurements performed on a 1.4MW induction machine with different emulated insulation conditions verify the applicability of the proposed method. The emulated insulation degradation cases tested are detectable and show a monotonic increasing tendency for increasing winding capacitance values. The influence of current slope which is induced by the machines fundamental wave behavior was tested and deviations in the slope estimation process were analyzed. A slope estimation algorithm suitable for real-time applications was tested and proven to deliver accurate results. It has to be stressed that the presented instulation monitoring method is a practical realization of patent (AT511807 B1), applied to the practical restrictions in traction drives.

ACKNOWLEDGMENT

The work to this investigation was supported and funded by the Austrian Research Promotion Agency (FFG) under project number 838478.

The authors want to thank Bombardier Transportation Switzerland (GSC/PPC-CoE2, head M. Joerg), and Bombardier Transportation Austria GmbH (GSC/PPC - Drives; electrical calculation group) for the generous support. Further the authors want to thank Product Development GSC/PPC Drives (M. Bazant) for PDev funding and feedback as well as Mr. Baro (GSC/PPC-Drives Global Engineering Head) for the great support. Thanks also goes to LEM - Company (especially Mr. W. Teppan) and National Instruments Austria (G. Stefan) for the cooperation and the generous support.

REFERENCES

[1] IEEE Committee Report; "Report of large motor reliability survey of industrial and commercial installation, Part I," *IEEE Transactions on Industry Applications*, vol.21, no.4, pp.853–864, 1985

[2] IEEE Committee Report; "Report of large motor reliability survey of industrial and commercial installation, Part II," *IEEE Transactions on Industry Applications,* vol.21, no.4, pp.865–872, 1985

[3] G. C. Stone, E. E. Boulter, I. Culbert, and H. Dhirani, "Electrical Insulation for Rotating Machines". *IEEE Press*, 2004

[4] IEEE Recommended Practice for Testing Insulation Resistance of Electric Machinery - Redline," *IEEE Std 43-2013 (Revision of IEEE Std 43-2000) - Redline* , vol., no., pp.1,75, March 6 2014

[5] IEEE Recommended Practice for Measurement of Power Factor Tip-Up of Electric Machinery Stator Coil Insulation," *IEEE Std 286-2000 , vol., no*., pp.i,29, 2001

[6] Farahani, M.; Borsi, H.; Gockenbach, E.; "Study of capacitance and dissipation factor tip-up to evaluate the condition of insulating systems for high voltage rotating machines," *Electrical Engineering*, vol.89, no.4, pp.263-270, 2007

[7] Farahani, M.; Gockenbach, E.; Borsi, H.; Schaefer, K.; Kaufhold, M.; "Behavior of machine insulation systems subjected to accelerated thermal aging test," *IEEE Transactions on Dielectrics and Electrical Insulation*, vol.17, no.5, pp.1364-1372, 2010

[8] Perisse, F.; Werynski, P.; Roger, D., "A New Method for AC Machine Turn Insulation Diagnostic Based on High Frequency Resonances," *Dielectrics and Electrical Insulation, IEEE Transactions on* , vol.14, no.5, pp.1308,1315, October 2007

[9] Kim, H.D.; Yang, J; Cho, J.; Lee, S.B.; Yoo, J.-Y.; "An Advanced Stator Winding Insulation Quality Assessment Technique for Inverter-Fed Machines," *IEEE Trans. on Ind. Appl.*, vol.44, no.2, pp.555-564, (Mar./Apr. 2008)

[10] Peroutka, Z., "Requirements for insulation system of motors fed by modern voltage source converters," *Power Electronics Specialists Conference, 2004. PESC 04. 2004 IEEE 35th Annual* , vol.6, no., pp.4383,4389 Vol.6, 20-25 June 2004

[11] Toliyat, Hamid A., et al. "Electric Machines: Modeling, Condition Monitoring, and Fault Diagnosis". *CRC Press*, 2012

[12] Jinkyu Yang; Jintae Cho; Sang-Bin Lee; Ji-Yoon Yoo, "An Advanced Stator Winding Insulation Quality Assessment Technique for Inverter-fed Machines," *Industry Applications Conference, 2006. 41st IAS Annual Meeting. Conference Record of the 2006 IEEE* , vol.3, no., pp.1562,1569, 8-12 Oct. 2006

[13] Nussbaumer, P.; Mitteregger, A.; Wolbank, T.M., "Online detection of insulation degradation in inverter fed drive systems based on high frequency current sampling," *IECON 2011 - 37th Annual Conference on IEEE Industrial Electronics Society* , vol., no., pp.1954,1959, 7-10 Nov. 2011

[14] Nussbaumer, P.; Wolbank, T.M.; Vogelsberger, M.A., "Sensitivity analysis of insulation state indicator in dependence of sampling rate and bit resolution to define hardware requirements," *Industrial Technology (ICIT), 2013 IEEE International Conference*, vol., no., pp.392,397, 25-28 Feb. 2013

[15] Nussbaumer, P.; Wolbank, T.M.; Vogelsberger, M.A, "Separation of disturbing influences on induction machine's high-frequency behavior to ensure accurate insulation condition monitoring," *Applied Power Electronics Conference and Exposition (APEC), 2013 Twenty-Eighth Annual IEEE* , vol., no., pp.1158,1163, 17-21 March 2013

[16] Zoeller, C.; Vogelsberger, M.A.; Nussbaumer, P.; Wolbank, T.M.; "Insulation monitoring of three phase inverter-fed ac machines based on two current sensors only" *21st International Conference on electrical machines ICEM 2014*, unpublished